NUMERICAL STUDY OF THE SHAPE EFFECT IN THE CERAMIC BASED BALLISTIC PANELS

Andrzej Morka, Beata Jackowska, Tadeusz Niezgoda

Military University of Technology
Gen. S. Kaliskiego St. 2, 00-908 Warsaw, Poland
tel.: +48 22 6837610, fax: +48 22 683 9355
e-mail: amorka@wat.edu.pl

Abstract

The numerical investigations have been performed to determine the front surface shape effect in the ceramic based armour systems. Different shapes of ceramic elements were analyzed, including hemispheres and pyramids, with respect to standard flat tiles. The influence of the impact point location was also under considerations.

The Computer simulations were performed with the Element Free Galerkin Method (EFG) implemented in LS-DYNA code. An impact of the 14.5x118mm B32 armour piercing projectile on the Al2O3 different shape elements backed by 7017 aluminium alloy plate was analyzed. Full 3D models of the projectile and targets were developed with strain rate and temperature dependent material constitutive relations. The models of the projectile, ceramic and aluminium alloy targets were validated with utilization of the experimental data found in literature.

The obtained results confirm, the preliminary presumptions, that the shape of the front surface can play significant role in the overall ballistic resistance of the panel. Particularly projectile-target initial contact area seems to be important factor as showed by impact point location analysis. The conclusions presented in this paper can be applied to develop modern impact protection panels where the appropriate balance between the mass and protection level must be accomplished.

Keywords: computational mechanics, impact problem, armour perforation, ballistic resistance, ceramic armour

1. Introduction

The paper concerns research and development on the modern, ceramic-based, protective layers, which are used in the armour of tanks, combat vehicles and aeroplanes. The ceramic panels are also adapted to bullet proof vests. These elements have three basic, very important features: hardness, brittleness and small mass density. A task of ceramic panels is reduction and dispersion of localized kinetic energy before a projectile or fragment approaches the interior of protected object. A hard ceramics cause that projectile is crumbled, while cracked ceramics disperse impact energy to the sides. As a result projectile decelerates remarkably or fully stops. Currently, the ceramic-based armours (e.g. CAWA-1) are used as a protection against 7.62 mm, 12.7 mm and 14.5 mm Armour Piercing (AP) projectiles [10].

In Al_2O_3 armours different shapes of ceramic elements are applied, e.g. square, rectangular, hexagonal. Generally armour plates have flat frontal surface, but more and more often possibility of convex or concave frontal surface panels usage is mentioned. In this paper influence of frontal surface's shape on armour effectiveness is discussed. Different shapes of the ceramic frontal surfaces were analyzed, including hemispheres and pyramids, with respect to standard flat tiles. Every case was numerically tested for several different points of projectile's impact. This makes possible to determine how convex or concave frontal surface influences the result of numerical analysis. The quantitative assessment was based on the calculated value of the kinetic energy versus time – $E_k(t)$ of the no destroyed part of projectile. The numerical simulations were performed with the Element Free Galerkin Method (EFG) implemented in LS-DYNA code [2, 7]. Three dimensional numerical models for each frontal surface idea were developed. The only considered were the perpendicular impacts because of the most dangerous expected results. An

explicit time integration algorithm was used as a method for the problem equations solution.

Currently the most expected ballistic resistance is related to the 14.5 x 118 mm B32 projectile. It ensures IV level of the ballistic protection according to the STANAG 4569 norm. Therefore this paper focuses on this kind of threat. That type of projectile consists of the soft metal jacket, incendiary material and the hard steel core. The last one part is the crucial element in penetration effectiveness. It carries overwhelming part of the projectile kinetic energy, more than 17 kJ with the impact velocity equals 910 m/s. The geometric characteristics of the hard steel core are presented in Fig. 1.
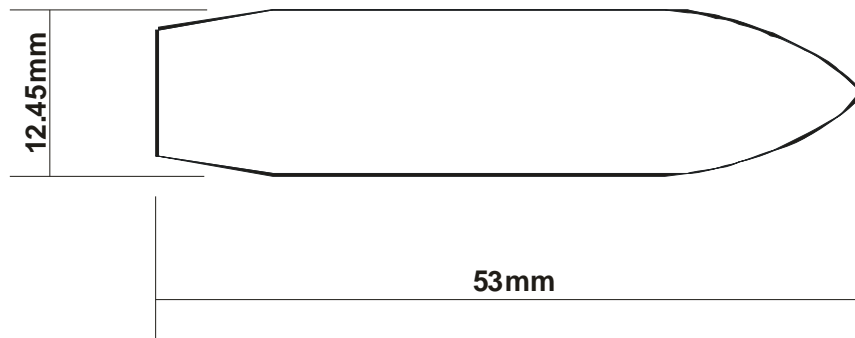

Fig. 1. A scheme of the 14.5x114mm B32 projectile's hard steel core

2. Description of the numerical model

For the purpose of the study of the frontal surface shape influence on the armour perforation several models of targets were built: flat, convex, and concave type, Fig. 2-4. All of them were made of ceramic Al_2O_3 and formed on the hexagonal base plate. Two kinds of convexities and concavities were considered. First, they were formed by regular pyramids with hexagonal base, Fig. 3. The length of the base edge equals 8 mm. The pyramids height also equals 8 mm. They are regularly spaced, starting from the centre of the target. Additionally, 8 mm thick ceramic hexagonal base plate with the edge length 50 mm was located behind the pyramids layer. That plate and pyramids formed a fully integrated single body. The second type of the rough surface was prepared very similar way, but the convexities/concavities were formed by hemispheres with diameter 16 mm regularly spaced, starting from the centre of the target, Fig. 4. It was assumed two reference cases with flat frontal surface 8 mm and 16 mm thick ceramic hexagonal tile, Fig. 2. The 10 mm thick 7017 aluminium alloy hexagonal plate was applied as a backing plate for all analyzed cases. Fig. 2-4 represent meshes of the numerical models consisting of three parts: the ceramic target backed by aluminium alloy plate and projectile's steel core. All of them were built with application of the four node tetrahedron solid element topology. The typical node to node distance was equal about 1mm in all cases of targets and projectiles. The total number of nodes per single case exceeded 200 k including 3.5 k of the nodes belonging to the steel core.

The excessive deformations often met in the perforation/penetration issues caused the choice a meshless method as the method for the problem solution. The Element Free Galerkin (EFG) method implemented in the LS-DYNA solver was selected. EFG only uses a set of nodal points describing a geometry of the body, no mesh in the classic sense is needed to define the problem [1, 7]. Nodes can be generated regularly or they can be locally concentrated. The connectivity between the nodes and the approximation functions are entirely constructed by the method [5]. It uses Moving Least Squares Approximation (MLSA) technique for the construction of the shape functions. The Galerkin weak form is applied to develop the discretized system of problem equations. Either a regular background mesh or a background cell structure is used for solving partial differential equations, in order to calculate the integrals in the weak form.
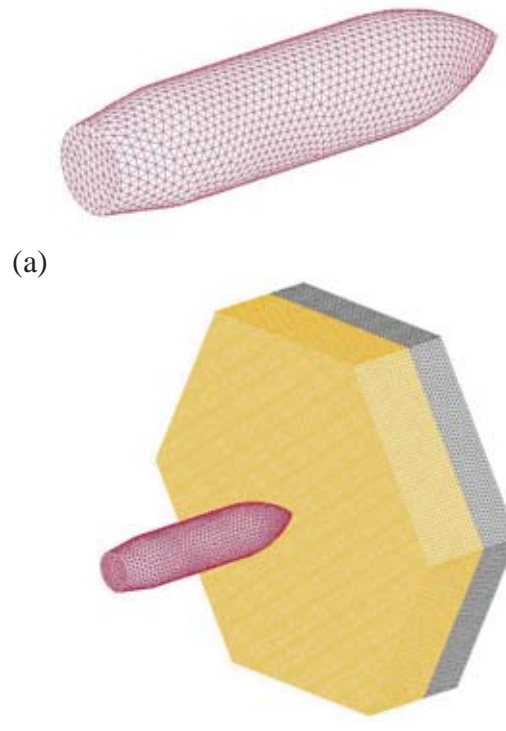
(a)

(b)

Fig. 2. A 3D view of the mesh and geometry of the 14.5x114mm B32 projectile's steel core (a), and the flat frontal surface case – reference case (b)
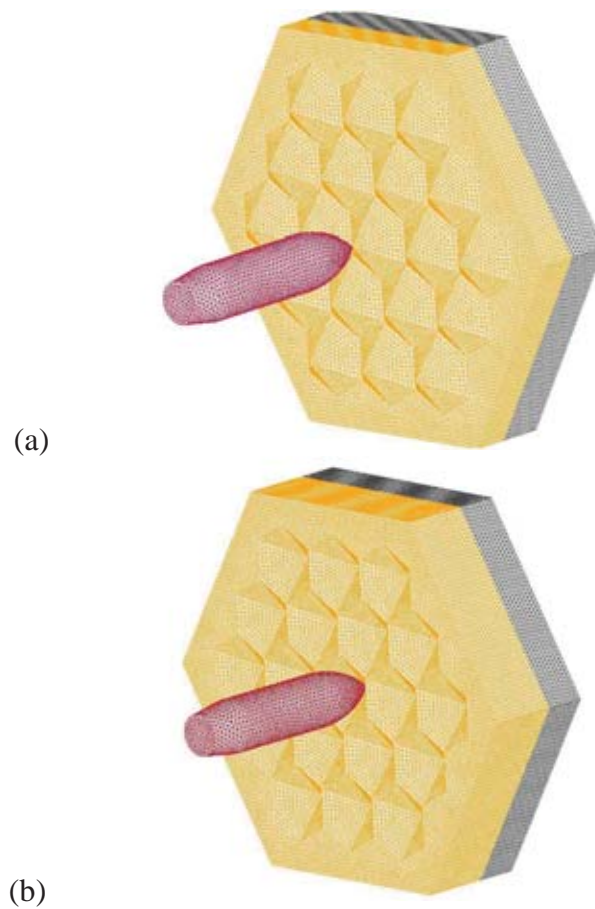

(a)

(b)

Fig. 3. A 3D view of the mesh and geometry of the pyramid type frontal surface, (a) convex case, (b) concave case
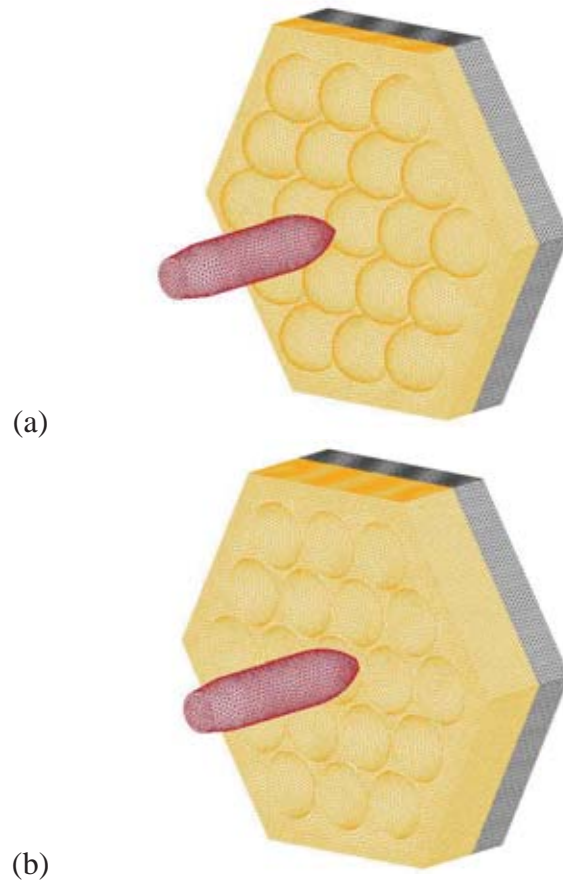
(a)

(b)

Fig. 4. A 3D view of the mesh and geometry of the hemisphere type frontal surface, (a) convex case, (b) concave case

The proper dynamic behaviour of metal alloys (hard steel, 7017 aluminium alloy) was realized by application of the Johnson-Cook (JC) constitutive model [6, 9] with the Gruneisen form of the Equation of State (EOS). The values of appropriate parameters are included in Tab. 1. The ceramic material was described by Johnson-Holmquist ceramic model (JH-2) [7, 5]. The material constants for high purity Al_2O_3 are presented in Tab. 2.

Tab. 1. Johnson-Cook model and Gruneisen EOS constants [7]

parameter	units	*hard steel*	*7017 Al alloy*
JC			
ρ	kg/m³	7790	2470
A	GPa	1.235	0.435
B	GPa	3.34	0.343
C		0.0114	0.01
m		0.94	1.0
n		0.89	0.41
T_m	K	1800	878
T_r	K	293	293
c_p	J/kgK	460	893
EOS			
c	m/s	4570	5240
S_1		1.49	1.4
S_2		0.0	0.0
S_3		0.0	0.0
γ_0		1.93	1.97
a		0.5	0.48

Tab. 2. Johnson-Holmquist model constants [7]

parameter	units	high purity Al_2O_3
JH-2		
ρ	kg/m³	3840
A		0.88
B		0.45
C		0.007
m		0.6
n		0.64
T	GPa	0.462
HEL	GPa	7.81
D_1		0.0125
D_2		0.7
EOS		
k_1	GPa	210
k_2	GPa	0.0
k_3	GPa	0.0

The initial condition was reduced to the given projectile velocity, 910 m/s. The boundary condition was assumed as the full fixing on the lateral edges of the backing hexagonal plate. The penalty type of contact was applied to characterize the model parts interaction, projectile/target and target/target. The eroding criteria thresholds, needed to reduce the calculation time, were defined at the validation stage. They are selected this way to minimize the result perturbations and keeping the acceptable agreement with the experimental data.

3. Validation of the numerical model

The developed numerical models were validated by exploitation of the data found in [8]. The authors of this paper carried out numerous of the experimental tests with the 12.7 x 108 mm B32 projectile impacting the 7017 aluminium alloy block and ceramic/aluminium alloy sets. They studied the depth of penetration in the 7017 alloy block for the different impact velocities and ceramic tile thickness. The results were presented in the form of tables.

Projectiles B32 type 14.5 x 118 mm and 12.7 x 108 mm are similar regarding their internal structure. Both of them are the Armour Piercing (AP) kind of munitions. The main element transmitting kinetic energy is a hard steel core in that case. The material characteristics of the hard steel (the core is made of) are the same for both types of projectiles. The general shape is similar also. The difference is only in the size and velocity. Therefore the numerical models were developed to reconstruct the experimental scenarios presented in [8]. They included: steel core of the 12.7 x 108 mm projectile, 20 x 20 x 40 cm block of 7071 aluminium alloy, ceramic tile 50 x 50 x (12)10 mm. The models component layout are showed in the Fig. 5a, 5b. The remaining assumptions of the model were left unchanged regarding the chapter 2. It was decided to apply a two mesh density regions in the target plates: very dense mesh close to the impact point, and coarse mesh elsewhere.
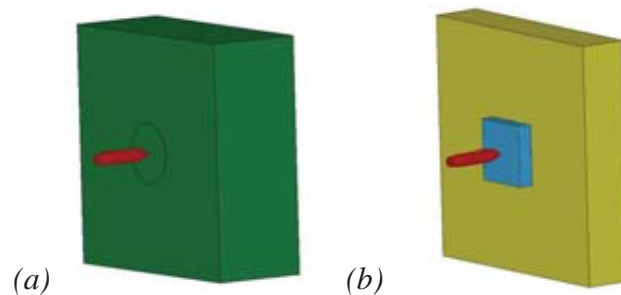

(a)   *(b)*

Fig. 5. Numerical models configuration for the validation stage. (a) penetration study of the 7017 aluminium alloy block, (b) penetration study of the ceramic/aluminium alloy set
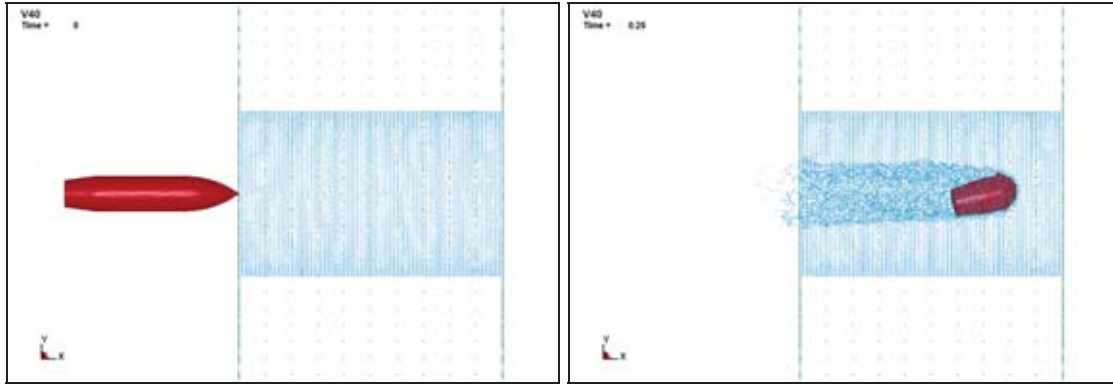
Fig. 6. Penetration of the 7017 aluminium alloy block by 12.7 x 108 B32 hard core. Impact velocity 829 m/s

Fig. 7. Penetration of the ceramic tile/aluminium alloy plate set by 12.7 x 108 B32 hard core. Impact velocity 840 m/s, ceramic tile thickness 10 mm

Tab. 3. Depth of penetration in the 7017 aluminium alloy block - validation and verification

	Experiment [mm]	Simulation [mm]	Error [%]
validation case - impact velocity 829 m/s	67	66	2
verification case - impact velocity 511 m/s	33	40	21

Tab. 4. Depth of penetration in the ceramic tile/7017 alloy plate set, impact velocity 840 m/s - validation and verification

	Experiment [mm]	Simulation [mm]	Error [%]
validation case - ceramic tile thickness 12 mm	5.8	5	14
verification case - ceramic tile thickness 10 mm	11.8	10	15

The initial and final stages of the penetration problems were depicted in the Fig. 5 and 6 for the 7017 alloy block alone and ceramic/aluminium alloy set suitably. These pictures present the side view with the impact point area enlarged. The dense and coarse meshes can be recognized. They are suitably connected together by applying specialized tied contact method available in the LS-DYNA solver. It is interesting the appearance of the distortions in the axial-symmetric movement of the projectile, Fig. 5, which is often observed in the experimental tests. The ceramic material fracture and fragmentation very similar to the real behaviour is showed in the Fig. 6. The quantitative analysis is based on the comparison of the Depth of Penetration (DoP) in aluminium alloy between numerical results and ballistic tests, Tab. 3 and 4. The validation cases were used to model behaviour improvement especially by defining the proper failing and eroding thresholds for ceramic and metals materials. The verification cases should confirm the valid model behaviour.

The obtained results, Tab. 3 and 4, showed that the maximal error in DoP reached 20% for both validation and verification cases, which is acceptable level for that kind of numerical analysis. It should be noticed that the DoP in the cases with ceramic tiles included, Tab. 4, was measured only in aluminium alloy plate.

4. Analysis of the results

The computer simulations were performed for the selected cases. High performance computing system based on the cluster architecture was used. It let to assign 4 to 8 CPUs per single job limiting the total computing time to reasonable level. Two cases with the flat frontal surface are treated as the reference cases and indicated respectively RC8 - 8 mm, RC16 - 16 mm thick ceramic tile. The convex pyramid-based cases are marked as CXP, while hemisphere-based CXH. For the concave occurrences they are CVP and CVH, adequately. During the calculations the time history of the projectile kinetic energy was stored with given time interval. Only the integral part of the projectile was considered. The specific value of this parameter was identified at the moment when the projectile completely perforates the backing plate. The accumulated data were used to conduct an assessment of the role of the shape factor in the global ballistic resistance of the ceramic-based armours. The different types of rough surfaces were compared each other as well as the location of the impact point was analysed for the given surface type. It was assumed, the projectile can hit three different representative points. The first point is in the centre of ceramics, the second between two pyramids (hemispheres), and the third is located half distance between the first and the second point. It is important that the performance of the system may differ, depending on the point the projectile hits.

The Fig. 8-11 present the influence of the impact point location on the projectile behaviour for each type of frontal surface referenced to the classical flat cases, black continuous (RC8 - 8 mm thick flat ceramic pate) and dashed (RC16 - 16 mm thick flat ceramic pate) lines. The curves describe time history of kinetic energy of the projectile's integral part. All cases were numbered as 1, 2 or 3 to indicate the successive impact point location: 1 - centre of ceramic tile, 2 - between two pyramids (hemispheres) and 3 - half distance between points 1 and 2. It is observed that in all occurrences the curves are located between two referencing cases. The better outcomes were obtained for centre impact (point 1) in cases of convex surface type, Fig. 8 and 10, while the concave surfaces behave good for 2nd and 3rd impact point location, Fig. 9 and 11. It is obviously related with the effective ceramic thickness ahead the projectile. The most promising result, i.e. minimal residual projectile's kinetic energy close to 7 kJ (the initial value was equal 17 kJ), was gained for the pyramid-based concave surface, CVP2, CVP3 in Fig. 9.
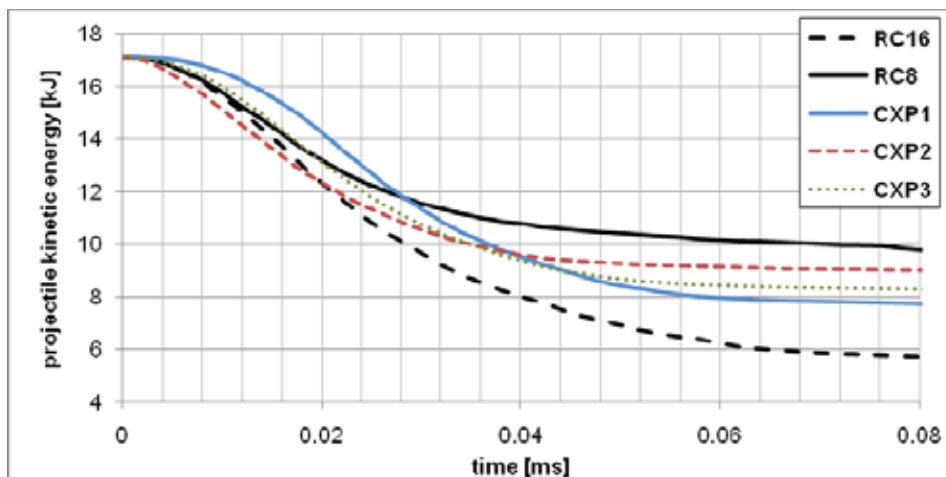

Fig. 8. Time history of the projectile kinetic energy. Impact point location analysis - convex pyramids case
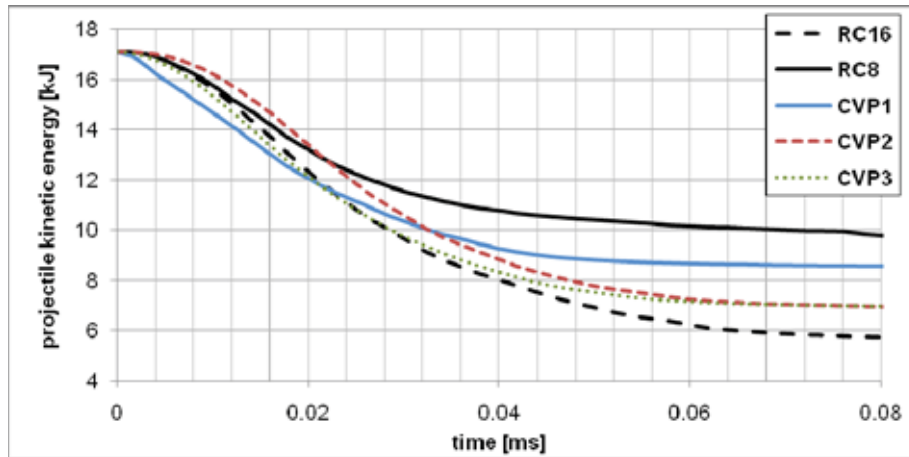
Fig. 9. Time history of the projectile kinetic energy. Impact point location analysis - concave pyramids case
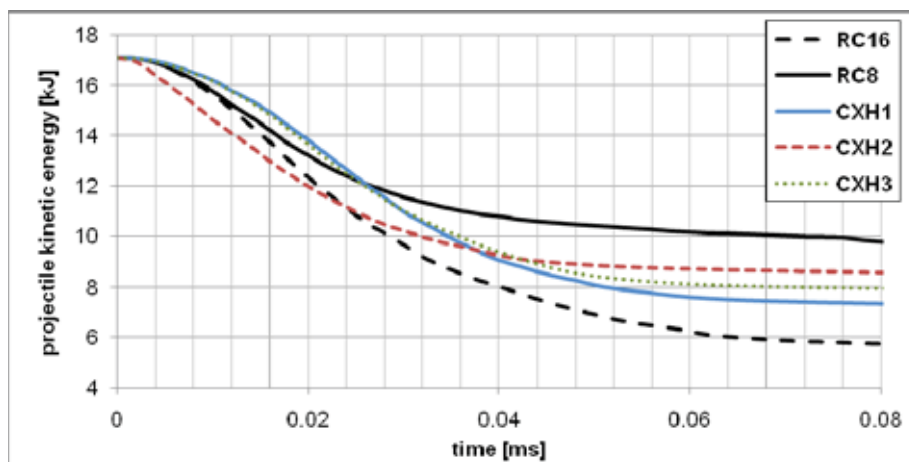

Fig. 10. Time history of the projectile kinetic energy. Impact point location analysis - convex hemispheres case
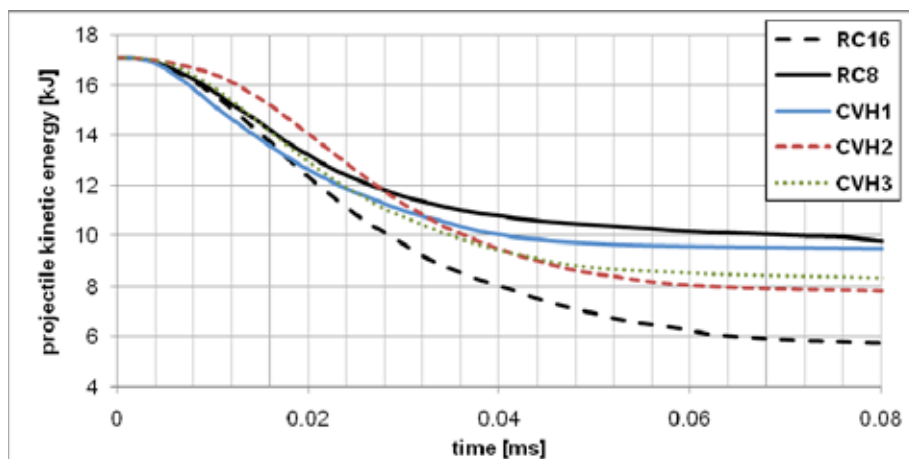

Fig. 11. Time history of the projectile kinetic energy. Impact point location analysis - concave hemispheres case

The residual kinetic energy of the integral part of the projectile for all analysed frontal surface types was depicted in Fig. 12. The comparison with the standard flat surface is also showed by the horizontal black lines marked RC8 and RC16. The shorter grey bar, the better result is procured. The pyramid-based convex surface (CVP2, CVP3 bars in Fig. 12) looks as the best option especially in case of 2nd and 3rd location of impact point, while the central impact in the hemisphere-based concave surface (CVH1) remains the worst case.
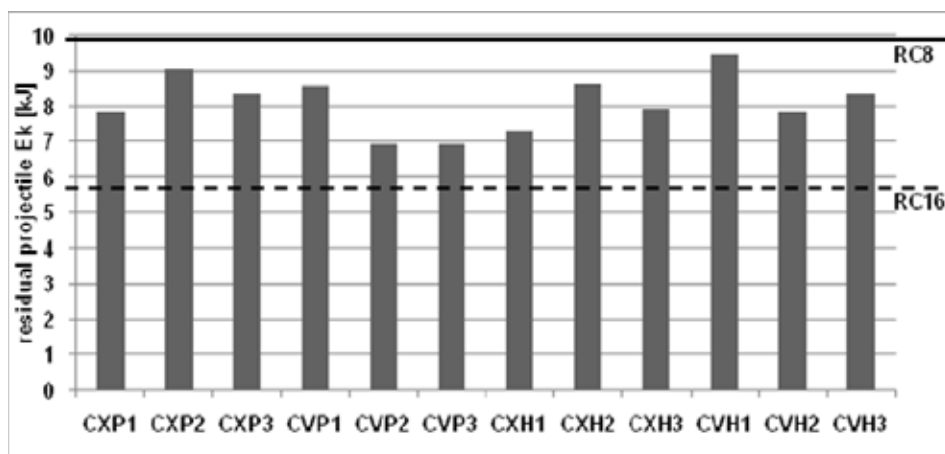
Fig. 12. The diagram of the ballistic effectiveness of the rough frontal surfaces with comparison to classic flat cases

5. Conclusions

The all performed calculations should provide reliable data because they are based on the good validated and verified numerical models. The studies conducted in this paper identified very interesting and promising dependencies with regard to role of the frontal surface shapes in the perforation problems.

It was showed that the effective ceramic thickness ahead the projectile is important, but not dominated. The surface shape is also very significant. The best outcomes with regard to the effectiveness of the projectile's restraining were observed for the pyramid-based concave cases especially when the impact point was located out of pyramids axes. This phenomenon is going to be investigated carefully in further works.

Additionally noticed effect consists in appearing meaningful value of the angular velocity of the residual projectile part during perforation process. It is observed for the 2nd location of the impact point and is common for all considered cases. This angular velocity can reach even 4rad/ms. That problem will be the subject of separate paper.

The conclusions presented in this paper can be applied to develop modern impact protection panels where the appropriate balance between the mass and protection level must be accomplished.

Acknowledgements

References

[1] Belytschko, T., Lu, Y. Y., Gu., L., *Element free Galerkin methods*, International Journal for Numerical Methods in Engineering, pp.229-256, 1994.

[2] Hallquist, J. O., *LS-DYNA Theory Manual*, Livermore Software Technology Corporation (LSTC), 2006.

[3] Holmquist, T. J., Templeton, D. W., Bishnoi, K. D., *Constitutive modeling of aluminium nitride for large strain, high-strain rate, and high - pressure applications*, International Journal of Impact Engineering, Vol. 25, pp. 211-231, Minneapolis 2001.

[4] Jaśkowiec, J., *Integracja metody elementów skończonych z bezelementową metodą Galerkina*, Proceedings of the XIII Scientific conference on numerical methods, Korbielów 2001.

[5] Kambur, C., *Assessment of Mesh-free Methods in LS-DYNA: Modeling of Barriers in Crash Simulation*, Master of Science Thesis, Institute for Structural Mechanics, Stuttgart 2004.

[6] Lee, M., Yoo, Y. H., *Analysis of ceramic/metal armour systems*, International Journal of Impact Engineering, Vol. 25, pp. 819-829, Seoul 2001.

[7] *LS-DYNA Keyword User's Manual*, Version 971, Livermore Software Technology Corporation (LSTC), 2007.

[8] Madhua, V., Ramanjaneyulua, K., Bhata, T. B., Gupta, N. K., *An experimental study of penetration resistance of ceramic armour subjected to projectile impact*, International Journal of Impact Engineering 32, pp. 337-350, 2005.

[9] Park, M., Yoo, J., Chung, D. T., *An optimization of a multi-layered plate under ballistic impact,* International Journal of Solids and Structures, Vol. 42, pp. 123-137, Seoul 2004.

[10] Wiśniewski, A., *Pancerze budowa, projektowanie i badanie,* Wydawnictwo Naukowo-Techniczne, Warszawa 2001.